SYNTHESIS, CHARACTERIZATION AND ELECTROCHEMICAL PROPERTIES OF rGO/NiCo$_2$S$_4$ NANOCOMPOSITE FOR SUPERCAPACITOR APPLICATION

Van Nguyen To[1], Minh Tuan Duong[1], Viet Linh Pham[1], Thi Vinh Hanh Le[1], Vu Sinh Tran[1], Xuan Duong Le[1], The Son Le[1], Manh Thao Pham[1,*]

[1]*Faculty of Physics and Chemical Engineering, Le Quy Don Technical University, Hanoi, Vietnam*

Abstract

In this study, rGO/NiCo$_2$S$_4$ composite materials were successfully synthesized by hydrothermal method. The properties of obtained materials were systematically characterized using XRD, SEM, EDX, and Raman techniques. The electrochemical performance of the materials was evaluated through cyclic voltammetry (CV) and Galvanostatic charge-discharge (GCD) measurements. The results show that the supercapacitor fabricated using rGO/NiCo$_2$O$_4$ could store energy using both double-layer and pseudocapacitor mechanisms with outstanding electrochemical properties. The specific capacity was up to over 2000 F/g at scanning speed of 10 mV/s or 1200 F/g at a current density of 1 A/g, which is 200-250% higher than the specific capacity of NiCo$_2$S$_4$ materials. This result demonstrates that rGO/NiCo$_2$S$_4$ material is a potential electrode material for supercapacitor applications.

Keywords: Supercapacitor; NiCo$_2$S$_4$; reduced graphene oxides.

1. Introduction

One of the promising future energy storage technologies is supercapacitor. It is well-known that supercapacitors have a lower energy density than batteries, while their power density is substantially higher. In addition, supercapacitors have several advantages over batteries, including longer lifetime and cheaper manufacturing costs. Of note, the electrochemical properties of supercapacitors are highly dependent on the electrode materials. Based on operating principles of supercapacitor energy storage, the electrode materials could be categorized into two types. The first type is the electrochemical double layer (EDLC) active materials, in which charge storage is dependent on the absorption/desorption of electrolyte ions at the interface between electrolyte and electrode. The second type is known as pseudo-capacitive (SP) active material, which facilitates the storage of electrical energy through a mechanism that

---

* Email: thaopm@gmail.com

involves reversible Faradaic redox reactions, and the intercalation/de-intercalation of ions or molecules into electrode structure [1]. Carbon-based materials, such as graphene and activated carbon, are typical examples of EDLC-operating materials, which have a high specific surface area and fast electrolytic ion exchange [1-4]. Meanwhile, transition metal oxide and transition metal sulfide are chosen as possible SP fabrication materials because of the variety of oxidation states present in their compounds, making them ideal for use as SP mechanism supercapacitor electrodes [5, 6].

Regarding the energy storage capacity, the pseudocapacitor materials have a higher specific capacity than that of EDLC materials, but their charging and discharging rates are significantly lower. Therefore, a number of studies have been conducted to enhance the charging and discharging rate of the pseudocapacitor materials. To overcome this issue, controlling composition and morphology of pseudocapacitor materials is considered as a simple and effective way. In a recent report, to create an electrodynamic material for hybrid supercapacitors, J. Cao et al. synthesized a mixture of nickel, cobalt, and manganese sulfide called NiCoMn-S [7]. As a result, the NiCoMn-S material exhibited superior electrochemical performance compared to nickel sulfide (Ni-S), cobalt-manganese sulfide (CoMn-S). Notably, the specific capacity of NiCoMn-S material was 1322 F/g at the current density of 1 A/g, and it remained unchanged at 880 F/g when subjected to a current density of 50 A/g. The synergistic effects of transition metals and the low resistance of the as-prepared electrode materials are the main reason for this superior electrochemical performance. In another research, B. T. Al-Abawi et al. did propose a strategy to control the morphology of nickel sulfide (NiS) on 3D Ni-foam (3DNF) for supercapacitor application [8]. By regulating sulfur precursor and thiourea concentration, different morphologies of NiS on 3DNF could be obtained including sheet-like structure, irregular sphere-shaped and uniform spherical morphology. The electrochemical measurements showed that the interconnected uniform sphere-shaped NiS on 3DNF had the highest specific capacitance of 694.0 F/g at 1 A/g with the excellent cycling stability of 88% after 6700 cycles. In short, composition and morphology often have a great impact on the electrochemical performance of electrode materials.

In another viewpoint, surface modification by coating or making composite with conductive materials such as polymers and carbon is also considered an effective strategy to improve electrochemical efficiency, especially charge-discharge rate [9, 10]. Souvik Ghosh et al. coated NiS_2 with carbon to simultaneously improve specific power, speed capacity and cycle efficiency [11]. This study found the optimal ratio between

carbon precursors and metal sulfides to create electrode materials with uniformly distributed particle size and lowest resistance, resulting in superior electrochemical performance. Specifically, the as-prepared electrode could provide an excellent specific capacitance of 2212 F/g with a current density of 2 A/g. Even at very high current density of 10 A/g the specific capacitance still reached 2000 F/g.

In this present work, we have successfully synthesized a mixture of nickel-cobalt sulfide ($NiCo_2S_4$) on rGO (rGO/$NiCo_2S_4$) by hydrothermal method. With the presence of rGO, the morphology $NiCo_2S_4$ was changed from rod-shape to granular shape. The characteristic properties of the composites were carefully and systematically investigated through XRD, Raman, SEM, and EDS analysis. Cyclic voltammetry (CV) and Galvanostatic charge-discharge (GCD) measurements were performed to evaluate the electrochemical performance of rGO/$NiCo_2S_4$. The results show that the rGO/$NiCo_2S_4$ material has an outstanding specific capacity of up to over 1000 F/g at a current density of 1 A/g, almost twice as high as that of $NiCo_2S_4$ (587 F/g at a current density of 587 F/g). 1 A/g); maintained 97.5% after 2000 cycles of charging-discharging continuously at a current density of 2 A/g. In short, we have demonstrated the superior energy storage performance of the rGO/$NiCo_2S_4$ nanocomposite, highlighting its potential as a high-performance electrode material for supercapacitor applications.

2. Experiments

2.1. Chemicals

Nickel (II) nitrate hexahydrate ($NiNO_3.6H_2O$); Cobalt (II) nitrate hexahydrate ($CoNO_3.6H_2O$); Thiourea (CH_4N_2S); Hydrochloric acid (HCl), Potassium hydroxide (KOH), Porous Nikel, Superconducting Carbon (Supper P), Polyvinylidene fluoride (PVDF); N-methyl-2-pyrrolidone (NMP). All chemicals were supplied by Aladdin Bio-Chem Technology Co., Ltd. and were of analytical purity, with no further purification required.

2.2. Synthesis of rGO/NiCo₂S₄ materials

Graphene oxide was synthesized by the improved Hummer method [12]. rGO/$NiCo_2S_4$ materials were then synthesized by hydrothermal method. Specifically, 4.42 g of GO solution was first dispersed in 25 mL water and stirred for 30 min at 80°C to get solution A. Next, dissolve 1 mmol of $Ni(NO_3)_2.6H_2O$ and 2 mmol $Co(NO_3)_2.6H_2O$ in 15 mL of H_2O and keep stirring for 30 min to obtain solution B. Following this, add solution B slowly to solution A under continuously magnetic stirring at 80°C for 2 h to obtain solution C. 4.5 mmol Thiourea and 2 mmol NH_4F were then added into solution C and stirred for 30 min to obtain solution D. Finally, solution

D was transferred into 50 mL Teflon reactor, reaction was carried out at 180°C for 12 h. After this, let it cool naturally. The obtained material was filtered, washed with water and ethanol, and dried in vacuum at 60°C for 12 h. For comparison, $NiCo_2S_4$ materials were synthesized by the same process as $rGO/NiCo_2S_4$ materials but without the presence of graphene oxide.

2.3. Material characterizations

The crystal structure, morphology and composition of the materials were determined using X-ray diffraction (XRD Bruker D8) with λ (Cu Kα2) = 1.54 Å, Raman spectroscopy (Horiba Jobin-Yvon LabRam HR800 Raman spectrometer) with the He-Ne laser of 632.8 nm as the excitation source, scanning electron microscopy (SEM, Hitachi S-48000) equipped with X-ray energy dispersive spectroscopy (EDS).

The electrochemical properties of the composites were evaluated by CV and GCD. All electrochemical measurements were conducted using Metrohm Autolab PGSTAT 302N equipped with a 3-electrode system consisting of working electrode, reference electrode (Ag/AgCl), counter electrode (platinum plate) in 3M KOH solution. To prepare the working electrode, a homogeneous mixture in NMP solvent is made by mixing active materials ($rGO/NiCo_2S_4$ or $NiCo_2S_4$), superconducting carbon and PDVF with a weight ratio of 8:1:1, respectively. The homogeneous mortar mixture was then pasted on the nickel foam sheet (0.5 cm × 0.5 cm) and dried in a vacuum oven at 60°C for 5 h. The mass of active material on the electrode was determined to be 0.4-0.6 mg.

3. Results and discussions

3.1. Structural and morphological characterization

As shown in Fig. 1, the observed diffraction peaks at 26.8, 31.6, 38.2, 50.2, and 55.2 were assigned for the lattice planes of (220), (311), (400), (511), and (440) of $NiCo_2S_4$ materials, respectively. The alignment of these peaks corresponds well to the characteristic cubic phase of $NiCo_2S_4$ (JCPDS # 20-0782), providing evidence that the synthesis of $NiCo_2S_4$ nanomaterials was successful [13] Fig. 1 shows that the characteristic peaks of $NiCo_2S_4$ appeared fully on the XRD spectrum of $rGO/NiCo_2S_4$ materials. However, the diffraction peaks of rGO were not observed, probably because of the small amount of rGO used. Furthermore, it is well-known that rGO usually processes a very board weak diffraction peak due to the low crystallinity of graphene [14, 15]. The XRD diffraction pattern also confirmed the high purity of obtained materials because there are no diffraction peaks of impurities observed.
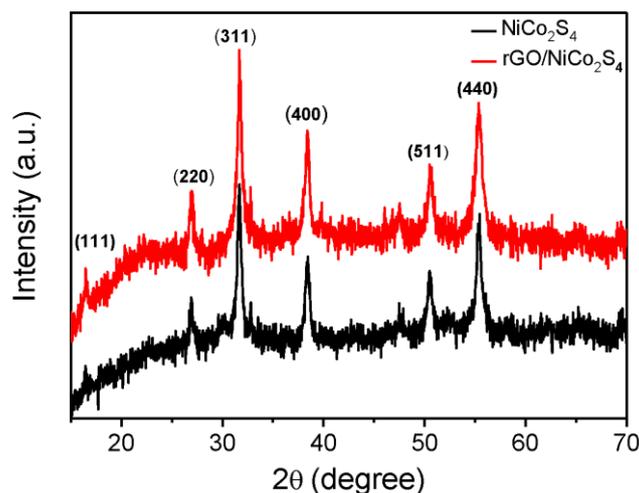
Fig. 1. The XRD pattern of NiCo$_2$S$_4$ and rGO/NiCo$_2$S$_4$.

Figure 2 shows the Raman spectra of NiCo$_2$S$_4$ and rGO/NiCo$_2$S$_4$ materials. The Raman spectrum of NiCo$_2$S$_4$ shows the the raman peaks at the low wavelength range of 300-700 cm^{-1}, which are identified as vibration modes of the A-S bond (A = Ni, Co). Similar signals are also observed in Raman spectrum of rGO/NiCo$_2$S$_4$ materials. Additionally, the Raman spectrum of rGO/NiCo$_2$S$_4$ also exhibits the D, G, and 2D bands of the rGO at about 1353, 1586, 2706 and 2918 cm^{-1}, respectively, which is consistent with the result of the previous studies [16]. Specifically, the D band corresponds to the vibrations of photons at the defects in the sp^2 plane. The G band corresponds to the scattering of photons in the sp^2 carbon plane and the prolonged vibration of the C-C bond. The 2D band at 2706 cm^{-1} demonstrates the synthesized rGO is multilayer [12]. Of note, the strength ratio between the D-band and G-band (D/G) is the basis for determining the degree of defect and the size of the sp^2 plane. This high ratio indicates that the degree of defect is large and the dimension of the sp^2 plane is reduced. Fig. 2 illustrates that the D/G ratio of rGO component in rGO/NiCo$_2$S$_4$ material is 1.65, which is larger than that of graphene synthesized using the physical methods (about 0.9 to 1.1). This is because the oxidation of graphite, in addition to dissection, is accompanied by destruction of the sp^2 plane leading to a reduced size of the sp^2 plane. Furthermore, the reduction of graphene oxide (GO) to rGO increases the defect density in the sp^2 plane [12]. In short, the results of Raman analysis agree with the XRD analysis, confirming that the rGO/NiCo$_2$S$_4$ composite materials are successfully synthesized composing of rGO and NiCo$_2$S$_4$.

44

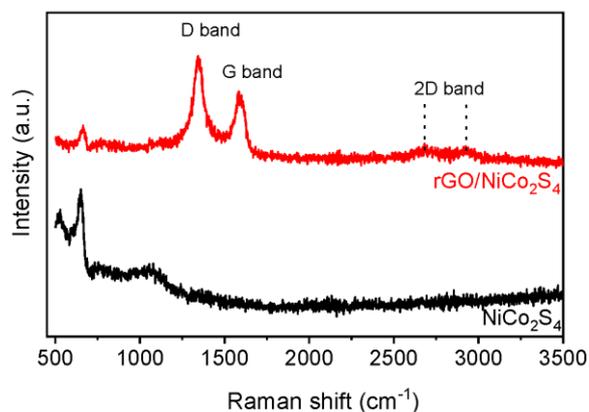*Fig. 2. The Raman spectra of $NiCo_2O_4$ and $rGO/NiCo_2O_4$.*

The morphology of the obtained materials was determined using SEM, which are shown in Fig. 3. The low and high magnification SEM images (Figs. 3a-3b) show that the $NiCo_2S_4$ had rod-shaped with the aspect ratio of about 50×500 nm. Interestingly, with the presence of rGO during synthezing process, $NiCo_2S_4$ was grown differently, which had the uniform granular shape with a size of about 50 nm (Figs. 3c-3d). The reason is that when nickel and cobalt precursors were added to the rGO dispersion, the graphene surface adsorbed Ni^{2+} and Co^{2+} cations through electrostatic interaction. During the hydrothermal procedure, graphene nanosheets with a large specific surface area acted as a deposition matrix for $NiCo_2S_4$ nanoparticles due to their ability to provide numerous nucleation sites, based on the theory of heteromorphic nuclei [17, 18]. Moreover, graphene nanosheets contain a unique structure with abundant oxygen-containing functional groups and high binding energy, resulting in the formation of nanoparticles in the composite [19]. The incorporation of a graphene network into the composite is expected to significantly enhance its electrical conductivity, which consequently improve the electrochemical perfomance of supercapacitor electrode. Notably, the rGO layer was clearly observed and resembles crumpled paper, which is probably because GO was synthesized using the strong oxidizing agent and the formation process was affected by agitation.

The chemical composition of the asprepared materials was investigated using EDS analysis. Fig. 4 shows the existence of Ni, Co, S and O in $NiCo_2S_4$ nanomaterials, while $rGO/NiCo_2S_4$ materials shows the signal of Ni, Co, S, O and C. Of note, the presence of O element in both $NiCo_2S_4$ and $rGO/NiCo_2S_4$ materials was probably because of the absorption of moisture during sample preparation. The atomic composition ratios of Ni, Co, and S in $NiCo_2S_4$ and $rGO/NiCo_2S_4$ materials are close to the empirical formula of $NiCo_2S_4$.
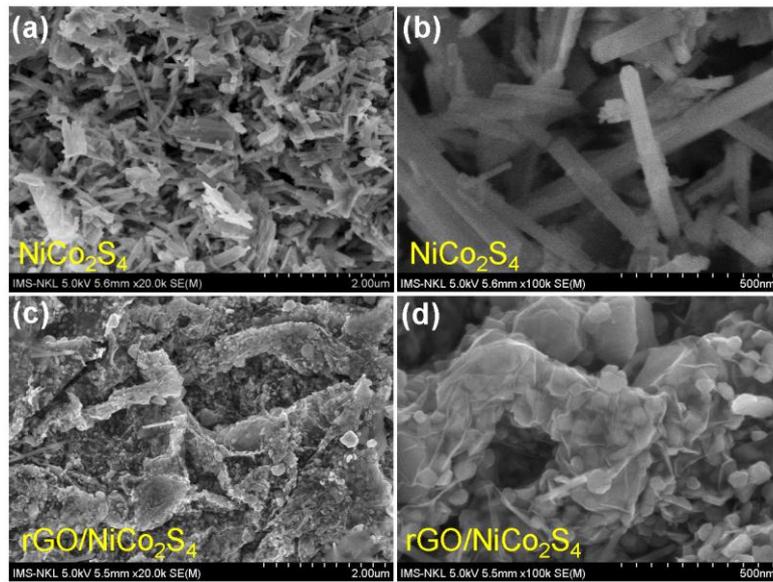
Fig. 3. The SEM images at (a) low and (b) high magnification of NiCo₂S₄ and SEM images at (c) low and (d) high magnification of rGO/NiCo₂S₄.
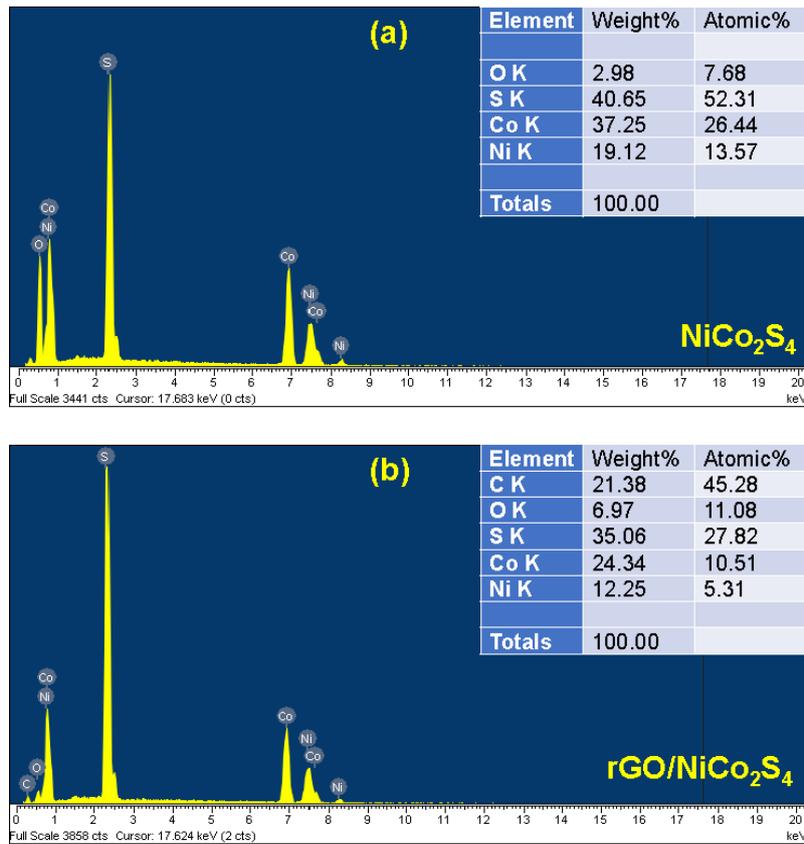

Element	Weight%	Atomic%
O K	2.98	7.68
S K	40.65	52.31
Co K	37.25	26.44
Ni K	19.12	13.57
Totals	100.00	

Element	Weight%	Atomic%
C K	21.38	45.28
O K	6.97	11.08
S K	35.06	27.82
Co K	24.34	10.51
Ni K	12.25	5.31
Totals	100.00	

Fig. 4. EDS analysis of (a) NiCo₂S₄ and (b) rGO/NiCo₂S₄.

3.2. Electrochemical properties

The mechanism and energy storage capacity of the $NiCo_2S_4$ and rGO/ $NiCo_2S_4$ were determined using CV scanning at the applied voltage ranging from 0 to 0.5 V and different scanning speeds of 10, 20, 40, 60, 80 and 100 mV/s. Fig. 5a shows the CV curve of rGO/ $NiCo_2S_4$ exhibits larger area compared to that of $NiCo_2S_4$, suggesting that the electrical energy storage capacity of rGO/$NiCo_2S_4$ material is higher. The redox peaks were clearly observed in both obtained materials, which indicates redox reaction would play an important role in energy storage mechanisms. The pair of redox peaks in the CV curve of $NiCo_2S_4$ and rGO/$NiCo_2S_4$ were determined to correspond to the Fraday reaction between M-S/M-S-OH (where M is Ni, Co) [20]. Figs. 5b-5c show the CV curves of $NiCo_2S_4$ and rGO/$NiCo_2S_4$ at different scanning rates, where the redox peaks of the materials are not shifted when the scanning speed is increased. This is evidence that the electrochemical reaction occurs on the surface at a fast rate, without electrode polarization and the process is almost ideally reversible [21].
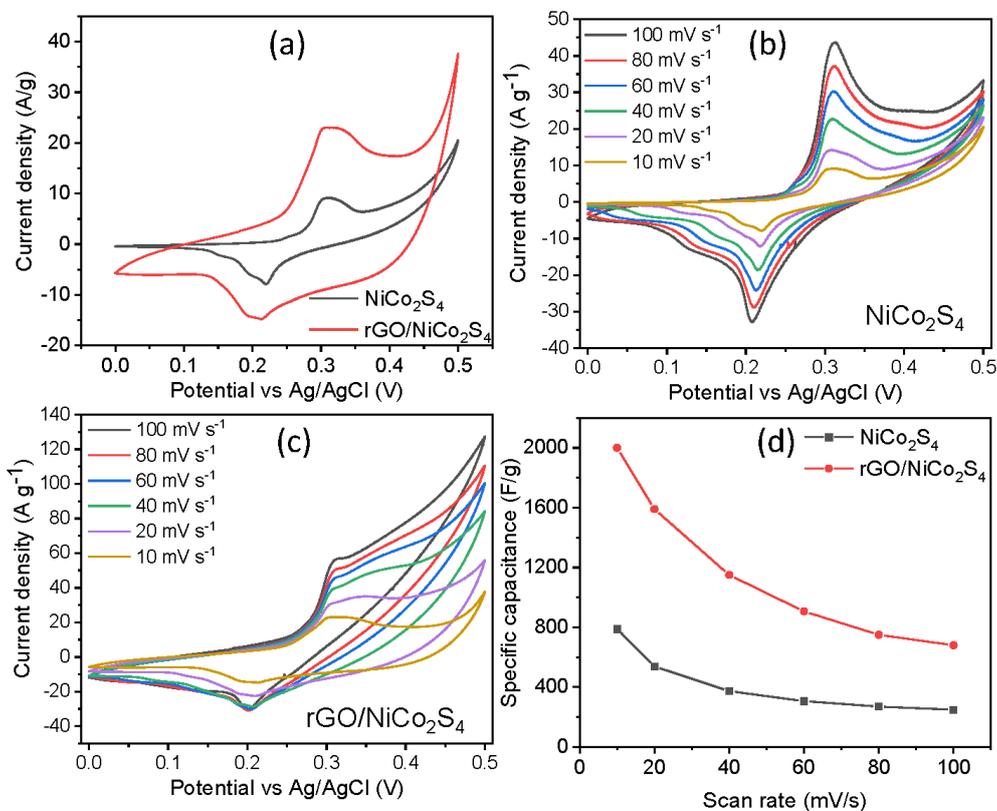

Fig. 5. (a) The cyclic voltammetry curves of NiCo₂S₄ and rGO/NiCo₂S₄ at the scanning rate of 10 mV/s; The cyclic voltammetry of (b) NiCo₂S₄ and (c) rGO/NiCo₂S₄ at different scanning rates; (d) The calculated specific capacities at different scanning rates.

47

The specific capacity of the material was determined from the cyclic voltammetry curves. The result shown in Fig. 5d indicates that the specific capacities are decreased with increasing scanning speed, which is related to the nature of the redox-based energy storage process limited by the reaction kinetics. By comparing storage capacity at the same scanning speed, rGO/NiCo$_2$S$_4$ materials exhibited a higher specific capacity than that of electrode materials fabricated using NiCo$_2$S$_4$ materials only. Specifically, the rGO/NiCo$_2$S$_4$ material had a maximum net capacity of 2000 F/g at 10 mV/s, which is 250% higher than that of NiCo$_2$S$_4$ (800 F/g).
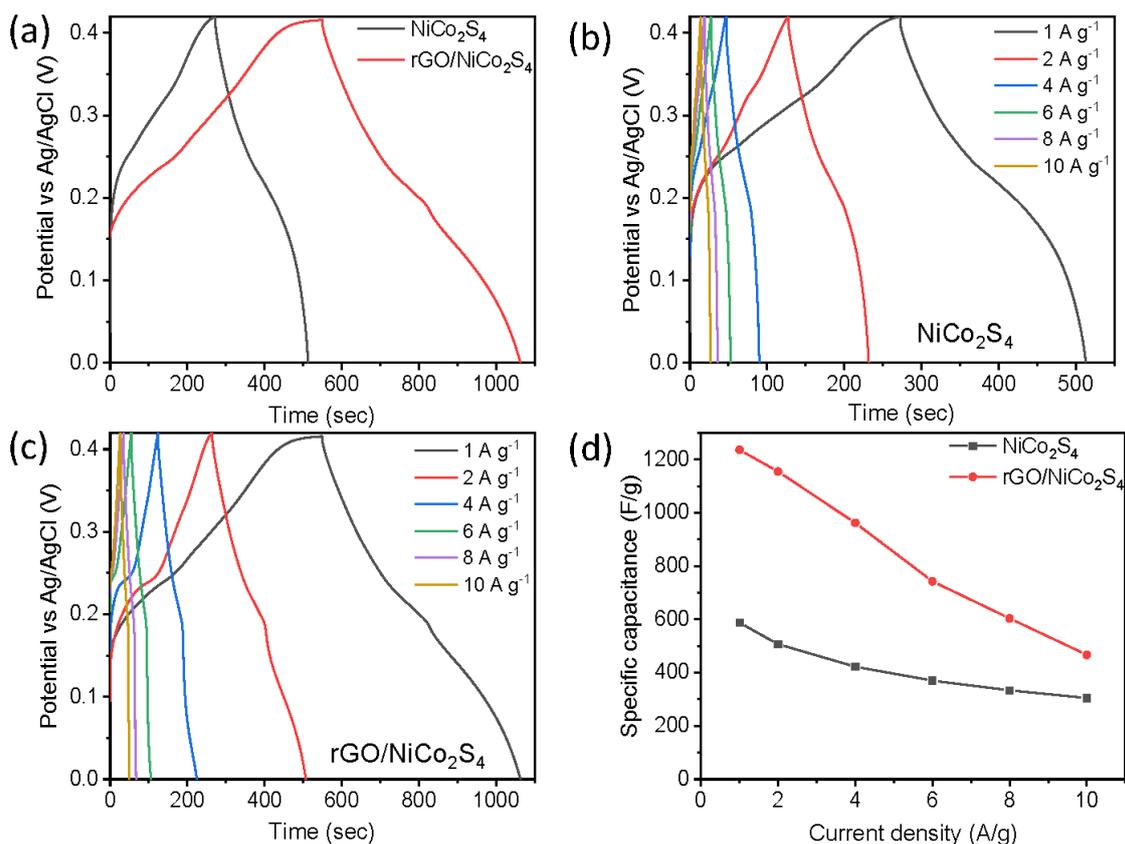

Fig. 6. (a) The GCD line of NiCo$_2$S$_4$ and rGO/NiCo$_2$S$_4$ at 1 A/g; The GCD line of (b) NiCo2S4 and (c) rGO/NiCo$_2$S$_4$ at different current density; (d) the calculated specific capacity of NiCo$_2$S$_4$ and rGO/NiCo$_2$S$_4$ at different current density.

GCD analysis for all material samples was performed in 3M KOH solution with current densities from 1 to 10 A/g while the applied voltage varied from 0 to 0.42 V. Fig. 6a shows the GCD curve of NiCo$_2$S$_4$ and rGO/NiCo$_2$S$_4$ materials at a current density of 1 A/g, which indicates that the charge-discharge time of rGO/NiCo$_2$S$_4$ materials took longer corresponding to the higher specific capacity. Figs. 6b and 6c show that all GCD lines have a voltage plateau (horizontal part) on the charge and

48

discharge lines at the voltage range corresponding to the redox peak observed on the CV line. The concordance of observed results on CV and GCD curves is an important basis to confirm that the energy storage mechanism of all materials is based on redox reaction. The specific capacities of the materials are calculated from the GCD curves shown in Fig. 6d. Like the CV analysis results, due to the limitation of the reaction kinetics, the specific capacities of all materials decrease with increasing charge-discharge current density from 1 to 10 A/g. Specifically, the maximum/minimum specific capacities of $NiCo_2S_4$ and $rGO/NiCo_2S_4$ materials are 578/304 and 1210/560 F/g, respectively. The superiority in energy storage capacity of $rGO/NiCo_2S_4$ materials over $NiCo_2S_4$ materials was determined due to the simultaneous resonance effect of both EDLC and PS energy storage mechanisms in $rGO/NiCo_2S_4$ materials.

Finally, the electrode performance of $rGO/NiCo_2S_4$ in our study, as demonstrated in Table 1, is comparable to other studies that utilized $NiCo_2S_4$ and their composite with carbon or graphene.

Table 1. Comparison of electrochemical properties of electrode materials ultilizing
$NiCo_2S_4$ and their composite with carbon or graphene

Electrode materials	Methods	Electrolyte	C_s	Reference
$NiCo_2S_4$	Hydrothemal	1M KOH	1000 F g^{-1} at 1 A g^{-1}	[22]
Carbon@$NiCo_2S_4$-H	Hydrothemal	6M KOH	1455 F g^{-1} at 1 A g^{-1}	[23]
Carbon@$NiCo_2S_4$	Hydrothemal	6M KOH	738.9 F g^{-1} at 1 A g^{-1}	[23]
NiS/rGO composites	Hydrothermal	3M KOH	905.3 F g^{-1} at 0.5 A g^{-1}	[24]
$NiCo_2S_4$/GNS	Hydrothermal	1M KOH	1063 F g^{-1} at 2 A g^{-1}	[18]
$NiCo_2S_4$-rGO	Hydrothermal	6M KOH	1107 F g^{-1} at 1 A g^{-1}	[25]
Sandwich-type $NiCo_2S_4$@rGO	Hydrothermal	2M KOH	2003 F g^{-1} at 1 A g^{-1}	[26]
$NiCo_2S_4$@rGO/rGO film electrode	Hydrothermal	6M KOH	1100.0 F g^{-1} at 1 A g^{-1}	[27]
$NiCo_2S_4$@$NiCo_2O_4$ core@ Shell on rGO sheet	Hydrothermal	6M KOH	1590.0 F g^{-1} at 5 A g^{-1}	[28]
$NiCo_2S_4$/rGO	Hydrothermal	2M KOH	963 F g^{-1} at 1 A g^{-1}	[29]
$rGO/NiCo_2S_4$	Solvothermal	3M KOH	1345 F g^{-1} at 2 A g^{-1}	This work

4. Conclusion

In this study, rGO/NiCo$_2$S$_4$ composite was successfully synthesized using hydrothermal reaction. Thanks to the resonance effect of EDLC and PS mechanism, rGO/NiCo$_2$S$_4$ composite had superior electrochemical properties compared to that of the single-component NiCo$_2$S$_4$. Consequently, rGO/NiCo$_2$S$_4$ composite had a maximum specific capacity of up to 2000 F/g at a scan rate of 10 mV/s or 1200 F/g at a current density of 1 A/g, which is double of that of NiCo$_2$S$_4$. Based on these results, it is suggested that rGO/NiCo$_2$S$_4$ composite is a potential material for supercapacitor electrode applications.

Acknowledgement

References

[1]   N. Kumar, S.-B. Kim, S. -Y. Lee, and S. -J. Park, "Recent Advanced Supercapacitor: A Review of Storage Mechanisms, Electrode Materials, Modification, and Perspectives*", Nanomaterials*, Vol. 12, p. 3708, 2022, DOI: 10.3390/nano12203708

[2]   K. Kraiwattanawong, "A review on the development of a porous carbon-based as modeling materials for electric double layer capacitors", *Arabian Journal of Chemistry*, Vol. 15, p. 103625, 2022, DOI: https://doi.org/10.1016/j.arabjc.2021.103625

[3]   J. Á. Martín-Illán, L. Sierra, P. Ocón, and F. Zamora, "Electrochemical Double-Layer Capacitor based on Carbon@ Covalent Organic Framework Aerogels*", Angewandte Chemie International Edition*, Vol. 61, p. e202213106, 2022, DOI: https://doi.org/10.1002/anie.202213106

[4]   A. Daraghmeh, S. Hussain, A.U. Haq, I. Saadeddin, L. Servera, and J.M. Ruiz, "Carbon nanocomposite electrodes for electrical double layer capacitor*", Journal of Energy Storage*, Vol. 32, p. 101798, 2020, DOI: https://doi.org/10.1016/j.est.2020.101798

[5]   X. Zhu, "Recent advances of transition metal oxides and chalcogenides in pseudo-capacitors and hybrid capacitors: A review of structures, synthetic strategies, and mechanism studies", *Journal of Energy Storage*, Vol. 49, p. 104148, 2022, DOI: https://doi.org/10.1016/j.est.2022.104148

[6]   N. V. Nguyen, T. V. Tran, S. T. Luong, T. M. Pham, K. V. Nguyen, T. D. Vu, H. S. Nguyen, and N. V. To, "Facile Synthesis of a NiCo$_2$O$_4$ Nanoparticles Mesoporous Carbon Composite as Electrode Materials for Supercapacitor", *ChemistrySelect*, Vol. 5, pp. 7060-7068, 2020, DOI: https://doi.org/10.1002/slct.202001410

[7]   J. Cao, Y. Hu, Y. Zhu, H. Cao, M. Fan, C. Huang, K. Shu, M. He, and H.C. Chen, "Synthesis of mesoporous nickel-cobalt-manganese sulfides as electroactive materials for hybrid supercapacitors", *Chemical Engineering Journal*, Vol. 405, 2021, p. 126928, DOI: https://doi.org/10.1016/j.cej.2020.126928

[8] B. T. Al-Abawi, N. Parveen, and S. A. Ansari, "Controllable synthesis of sphere-shaped interconnected interlinked binder-free nickel sulfide@nickel foam for high-performance supercapacitor applications", *Scientific Reports*, Vol. 12, p. 14413, 2022, DOI: 10.1038/s41598-022-18728-1

[9] S. Suriyakumar, P. Bhardwaj, A. N. Grace, and A. M. Stephan, "Role of Polymers in Enhancing the Performance of Electrochemical Supercapacitors: A Review*", Batteries & Supercaps*, Vol. 4, pp. 571-584, 2021, DOI: https://doi.org/10.1002/batt.202000272

[10] K. Hareesh, B. Shateesh, R.P. Joshi, J. F. Williams, D. M. Phase, S. K. Haram, and S. D. Dhole, "Ultra high stable supercapacitance performance of conducting polymer coated MnO_2 nanorods/rGO nanocomposites", *RSC Advances*, Vol. 7, pp. 20027-20036, 2017, DOI: 10.1039/C7RA01743J

[11] S. Ghosh, J. Sharath Kumar, N. Chandra Murmu, R. Sankar Ganesh, H. Inokawa, and T. Kuila, "Development of carbon coated NiS_2 as positive electrode material for high performance asymmetric supercapacitor*", Composites Part B: Engineering*, Vol. 177, p. 107373, 2019, DOI: https://doi.org/10.1016/j.compositesb.2019.107373

[12] T. V. Thu, T. Van Nguyen, X. D. Le, T. S. Le, V. Van Thuy, T. Q. Huy, and Q. D. Truong, "Graphene-MnFe2O4-polypyrrole ternary hybrids with synergistic effect for supercapacitor electrode", *Electrochimica Acta*, Vol. 314, pp. 151-160, 2019, DOI: https://doi.org/10.1016/j.electacta.2019.05.042

[13] Y. W. Sui, Y. M. Zhang, P. H. Hou, J. Q. Qi, F. X. Wei, Y. Z. He, Q. K. Meng, and Z. Sun, "Three-dimensional NiCo2S4 nanosheets as high-performance electrodes materials for supercapacitors", *Journal of Materials Science*, Vol. 52, pp. 7100-7109, 2017, DOI: 10.1007/s10853-017-0942-8

[14] J. Prasad, A. K. Singh, K. K. Haldar, V. Gupta, and K. Singh, "Electromagnetic interference shielding effectiveness in 3D flower-like MoS_2-rGO/gadolinium-doped nanocomposites", *Journal of Alloys and Compounds*, Vol. 788, pp. 861-872, 2019, DOI: https://doi.org/10.1016/j.jallcom.2019.02.246

[15] H. -H. Huang, K. K. H. De Silva, G. R. A. Kumara, and M. Yoshimura, "Structural Evolution of Hydrothermally Derived Reduced Graphene Oxide", *Scientific Reports*, Vol. 8, p. 6849, 2018, DOI: 10.1038/s41598-018-25194-1

[16] N. M. S. Hidayah, W. -W. Liu, C. -W. Lai, N. Z. Noriman, C. -S. Khe, U. Hashim, and H. C. Lee, "Comparison on graphite, graphene oxide and reduced graphene oxide: Synthesis and characterization", AIP Conference Proceedings, Vol. 1892, p. 150002, 2017, DOI: 10.1063/1.5005764

[17] X. Y. Liu, "Heterogeneous nucleation or homogeneous nucleation?", The Journal of Chemical Physics, Vol. 112, pp. 9949-9955, 2000, DOI: 10.1063/1.481644

[18] X. Yang, H. Niu, H. Jiang, Z. Sun, Q. Wang, and F. Qu, "One-Step Synthesis of NiCo2S4/Graphene Composite for Asymmetric Supercapacitors with Superior Performances", ChemElectroChem, Vol. 5, pp. 1576-1585, 2018, DOI: https://doi.org/10.1002/celc.201800302

[19]   P. Ghosh, et al., "Insights on Defect-Mediated Heterogeneous Nucleation of Graphene on Copper", *The Journal of Physical Chemistry C*, Vol. 119, pp. 2513-2522, 2015, DOI: 10.1021/jp510556t.

[20]   T. Chen, Y. Tang, W. Guo, Y. Qiao, S. Yu, S. Mu, L. Wang, Y. Zhao, and F. Gao, "Synergistic effect of cobalt and nickel on the superior electrochemical performances of rGO anchored nickel cobalt binary sulfides", *Electrochimica Acta*, Vol. 212, pp. 294-302, 2016, DOI: https://doi.org/10.1016/j.electacta.2016.07.023.

[21]   P. Xu, et al., "Carbon Nanotube Fiber Based Stretchable Wire-Shaped Supercapacitors", Advanced Energy Materials, Vol. 4, p. 1300759, 2014, DOI: https://doi.org/10.1002/aenm.201300759.

[22]   D. Y. Kim, G. S. Ghodake, N.C. Maile, A. A. Kadam, D. Sung Lee, V. J. Fulari, and S. K. Shinde, "Chemical synthesis of hierarchical NiCo2S4 nanosheets like nanostructure on flexible foil for a high performance supercapacitor", *Scientific Reports*, Vol. 7, p. 9764, 2017, DOI: 10.1038/s41598-017-10218-z.

[23]   L. Li, Z. Dai, Y. Zhang, J. Yang, W. Huang, and X. Dong, "Carbon@NiCo2S4 nanorods: an excellent electrode material for supercapacitors", *RSC Advances*, Vol. 5, pp. 83408-83414, 2015, DOI: 10.1039/C5RA15022A.

[24]   J. Yang, X. Duan, W. Guo, D. Li, H. Zhang, and W. Zheng, "Electrochemical performances investigation of NiS/rGO composite as electrode material for supercapacitors", Nano Energy, Vol. 5, pp. 74-81, 2014, DOI: https://doi.org/10.1016/j.nanoen.2014.02.006.

[25]   Y. -M. Fan, Y. Liu, X. Liu, Y. Liu, and L. -Z. Fan, "Hierarchical porous NiCo2S4-rGO composites for high-performance supercapacitors", *Electrochimica Acta*, Vol. 249, pp. 1-8, 2017, DOI: https://doi.org/10.1016/j.electacta.2017.07.175.

[26]   F. Wang, G. Li, Q. Zhou, J. Zheng, C. Yang, and Q. Wang, "One-step hydrothermal synthesis of sandwich-type NiCo2S4@reduced graphene oxide composite as active electrode material for supercapacitors", *Applied Surface Science*, Vol. 425, pp. 180-187, 2017, DOI: https://doi.org/10.1016/j.apsusc.2017.07.016.

[27]   Y. Liu, D. Su, Z. Sang, X. Su, H. Chen, and X. Yan, "High-performance layered NiCo$_2$S$_4$@rGO/rGO film electrode for flexible electrochemical energy storage", *Electrochimica Acta*, Vol. 328, p. 135088, 2019, DOI: https://doi.org/10.1016/j.electacta.2019.135088.

[28]   A. Singh, S. K. Ojha, M. Singh, and A. K. Ojha, "Controlled synthesis of NiCo$_2$S$_4$@NiCo$_2$O$_4$ core@Shell nanostructured arrays decorated over the rGO sheets for high-performance asymmetric supercapacitor", *Electrochimica Acta*, Vol. 349, p. 136349, 2020, DOI: https://doi.org/10.1016/j.electacta.2020.136349.

[29]   H. -I. Hsiang, C. -H. She, and S. -H. Chung, "Materials and electrode designs of high-performance NiCo$_2$S$_4$/Reduced graphene oxide for supercapacitors", *Ceramics International*, Vol. 47, pp. 25942-25950, 2021, DOI: https://doi.org/10.1016/j.ceramint.2021.05.325.

TỔNG HỢP VÀ NGHIÊN CỨU TÍNH CHẤT ĐIỆN HÓA CỦA VẬT LIỆU COMPOSITE rGO/NiCo$_2$S$_4$ ỨNG DỤNG LÀM ĐIỆN CỰC SIÊU TỤ

Tô Văn Nguyện[a], Dương Minh Tuân[a], Phạm Việt Linh[a], Lê Thị Vinh Hạnh[a], Trần Vũ Sinh[a], Lê Xuân Dương[a], Lê Thế Sơn[a], Phạm Mạnh Thảo[a]

[a]*Khoa Hóa - Lý kỹ thuật, Đại học Kỹ thuật Lê Quý Đôn*

Tóm tắt: Trong nghiên cứu này, vật liệu composite rGO/NiCo$_2$S$_4$ được tổng hợp thành công bằng phương pháp thủy nhiệt. Các tính chất của vật liệu thu được được nghiên cứu một cách có hệ thống bằng các kỹ thuật XRD, SEM, EDX, Raman. Tính chất điện hóa của vật liệu được đánh giá thông qua phép đo điện thế tuần hoàn (CV) và phép đo phóng điện tĩnh điện (GCD). Kết quả cho thấy siêu tụ điện được chế tạo bằng rGO/NiCo$_2$O$_4$ có thể lưu trữ năng lượng bằng cả cơ chế hai lớp và giả tụ điện với các đặc tính điện hóa vượt trội. Dung lượng riêng lên tới hơn 2000 F/g ở tốc độ quét 10 mV/s hoặc 1200 F/g ở mật độ hiện tại 1 A/g, cao hơn 200-250% so với công suất riêng của vật liệu NiCo$_2$S$_4$. Kết quả này cho thấy vật liệu rGO/NiCo$_2$S$_4$ là vật liệu điện cực tiềm năng cho các ứng dụng siêu tụ điện.

Từ khóa: *Siêu tụ điện; NiCo$_2$S$_4$; graphen oxit.*

❑